

**TECHNISCHE  
UNIVERSITÄT  
DRESDEN**

---

---

# Title of Bachelor thesis

Bachelor-Arbeit  
zur Erlangung des Hochschulgrades  
Bachelor of Science  
im Bachelor-Studiengang Physik

vorgelegt von

EDGAR MARQUARDT  
geboren am 07.09.2002 in Leipzig

Institut für Kern- und Teilchenphysik  
Fakultät Physik  
Bereich Mathematik und Naturwissenschaften  
Technische Universität Dresden  
2025

Eingereicht am 05. Januar 2026

1. Gutachter: Prof. Dr. Ulrich Schramm
2. Gutachter: Prof. Dr. Thomas Cowan

# Summary

Abstract

English:

Abstract

Deutsch



# Contents

<b>1</b>	<b>Introduction</b>	<b>6</b>
1.1	Motivation: Laser wakefield acceleration (LWFA) . . . . .	6
1.2	The problem of Dephasing . . . . .	7
1.3	The Axiparabola . . . . .	7
1.4	Spatio-temporal control . . . . .	9
<b>2</b>	<b>Simulation tools</b>	<b>10</b>
2.1	Lasy . . . . .	10
2.2	openPMD . . . . .	10
2.3	PIConGPU . . . . .	10
2.4	Additional modules . . . . .	11
<b>3</b>	<b>Gaussian pulses in Lasy</b>	<b>16</b>
3.1	Testing Gaussian pulses . . . . .	16
3.2	Gaussian pulse and parabolic mirror . . . . .	17
<b>4</b>	<b>Lasy pulses in PIConGPU</b>	<b>19</b>
4.1	Courant-Friedrich-Levy (CFL) condition . . . . .	19
4.2	Comparative test with the Gauss laser . . . . .	20
<b>5</b>	<b>The flying focus laser</b>	<b>22</b>
5.1	Testing the radial group delay . . . . .	22
5.2	Testing the axiparabola . . . . .	23
5.3	The complete assembly . . . . .	26
5.4	Testing different propagators . . . . .	30
<b>6</b>	<b>Summary and Outlook</b>	<b>31</b>
6.1	Summary . . . . .	31
6.2	Outlook . . . . .	31
6.3	Code availability . . . . .	31
	<b>Bibliography</b>	<b>32</b>
	<b>List of Figures</b>	<b>34</b>

# Chapter 1

## Introduction

### 1.1 Motivation: Laser wakefield acceleration (LWFA)

Since the invention of LWFA by Tajima and Dawson [18] compact accelerators are a useful tool in radiation physics. It enables more labs to work with high energy electrons for their research. This in turn enables technologies using these electrons, for example free electron lasers which can generate laser pulses in otherwise unreachable frequency ranges. Our Group has used and researched them for a while now and is working on the cutting edge of this technology, see for example [6], [9] and [11].

LWFA works as follows: A laser is focused into a gas, usually hydrogen, where it needs to be intense enough to ionize the gas and push the electrons out of the way. In figure 1.1 this happens on the right of the laser pulse. Behind the laser they come back together which produces extreme electric fields on the order of several 100GV/m (see [7]) in the propagation direction of the laser. This accelerating field can be seen in figure 1.1 in blue. Because these fields can become up to 3 orders of magnitude stronger than a traditional radiofrequency accelerator cavity they can accelerate electrons to multiple GeV over a distance of just centimeters [7]. Figure 1.1 shows the electrons with a color gradient to show their energy. The yellow region is where the electron bunch is currently being accelerated by riding on the laser wakefield.

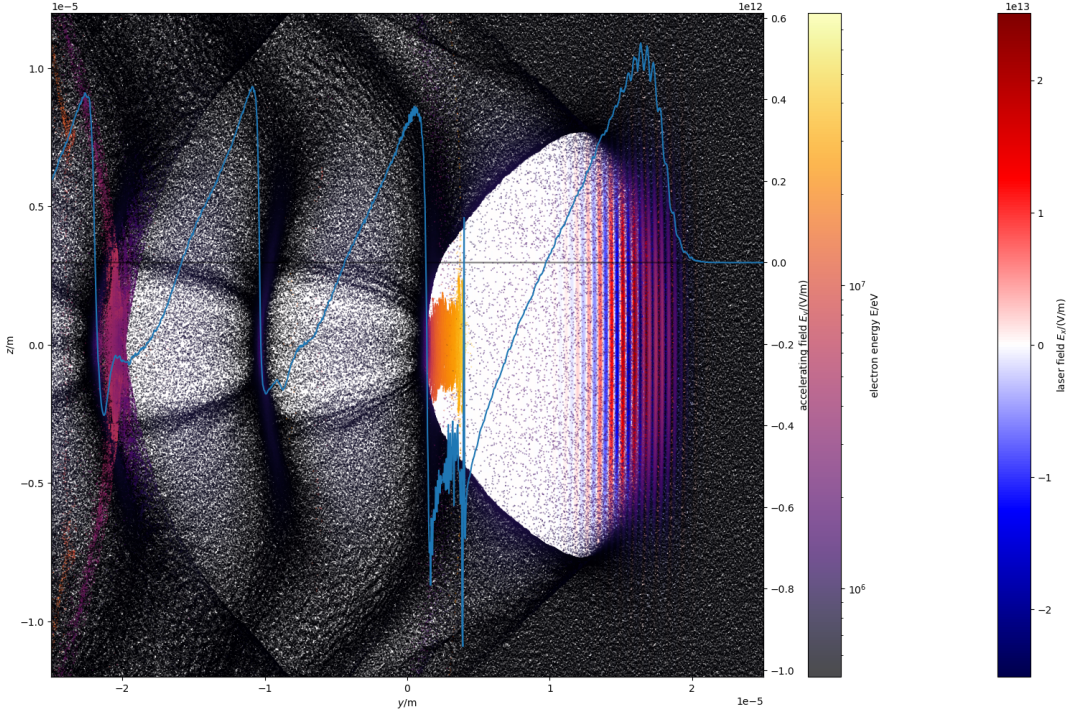


**Figure 1.1:** PIConGPU simulation of laser wakefield acceleration. Displayed are the electrons, colored according to their energy  $E$ , the electric field of the laser pulse  $E_x$  and the on-axis accelerating field  $E_y$  in blue.

## 1.2 The problem of Dephasing

LWFA is known to be facing three major problems: Depletion, Diffraction and Dephasing. Depletion happens, when the laser pulse driving the wake has given so much of its energy to the electrons that it can no longer drive the wake. Diffraction is the laser pulse getting out of focus and therefore losing the wake. Dephasing describes the process by which electrons are accelerated to velocities over the speed of light in the plasma. Because of the high fields in the wake of the laser pulse this happens after a few centimeters of acceleration. The electrons can now slowly approach the laser pulse until the field in the propagation direction reverses and no longer accelerates the electrons and instead decelerates them. In figure 1.1 this reversal can be seen to the left of the laser pulse. This effect puts an upper limit to the energy an electron can leave the acceleration region with. A common solution is to accelerate the electrons in multiple stages to increase the energy but this is complicated and inconvenient. Debus et al [7] have shown that it is possible to solve Dephasing (and also Depletion) by using two separate laser pulses with tilted wave fronts. However, this is complicated to achieve. According to Palastro et al [15] as well as Miller et al [13] Dephasing could also be solved using a so called flying focus setup. It is made out of a radial group delay echelon and an axiparabola.

## 1.3 The Axiparabola

In 2019 Smartsev et al proposed and tested a new optical device called the axiparabola [16]. It is a mirror shaped similarly to an off-axis parabola and is defined by three parameters: the nominal focal length  $f_0$ , the length of the focal region  $\delta$  and the radius  $R$ . An axiparabola does not only focus a pulse onto one specific point but onto a line on the optical axis of the length  $\delta$ . It achieves this by focusing

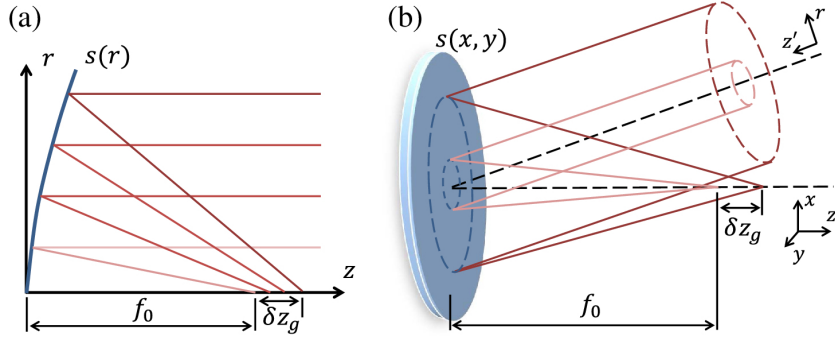


**Figure 1.2:** Schematic of how an axiparabola focuses light into the focal region. Rays close to the optical axis are focused to a focus length of  $f_0$  and rays far from the axis are focused closer to  $f_0 + \delta$ .  
(a) On-axis case, (b) off-axis case. Image taken from Smartsev et al[16].

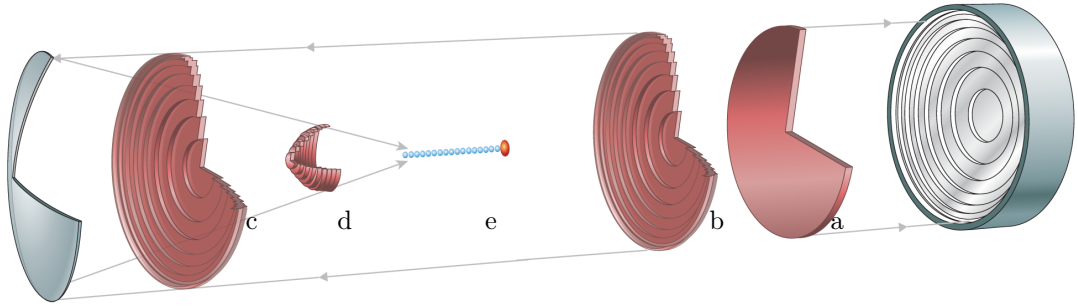


**Figure 1.3:** Schematic of the flying focus setup. A flat laser pulse (a) is first reflected by the radial group delay echelon (b). It imparts a time delay onto the pulse without aberrations. The pulse (c) is then reflected by the axiparabola, which focuses the pulse (d) into the focal region  $\delta$  (e), where it can theoretically drive a laser wakefield accelerator without dephasing. Image taken from Palastro et al [15].

the pulse to different focus lengths at different radii:

$$f(r) = f_0 + \delta \left( \frac{r}{R} \right)^2 \quad (1.1)$$

In figure 1.2 on the left side is shown, how this should be understood. The sag function describing the shape of the axiparabola looks as follows:

$$s_f(r) = \frac{1}{4f_0}r^2 - \frac{\delta}{8f_0^2 R^2}r^4 + \frac{\delta(R^2 + 8f_0\delta)}{96f_0^4 R^4}r^6 + \mathcal{O}(r^8)[16] \quad (1.2)$$

Ambat et al [4] also proposed a closed formula:

$$s_f(r) = \frac{R^2}{4\delta} \ln \left( 1 + \frac{\delta}{f_0} \left( \frac{r}{R} \right)^2 \right) \quad (1.3)$$

According to Ambat et al [4] the beam waist between  $f_0 < z < f_0 + \delta$  should follow roughly the relation

$$w(z) \approx \frac{\lambda_0 f_0}{\pi R} \sqrt{\frac{\delta}{z - f_0}}. \quad (1.4)$$

This can of course only apply at sufficient distance from  $f_0$ , because otherwise  $\lim_{z \rightarrow f_0} w(z) = \infty$ . The time when the focus reaches a distance  $z$  from the axiparabola is roughly:

$$t_f(z) \approx \frac{1}{c} \left( z + \frac{(z - f_0)R^2}{\delta \cdot 2z} - 2s_f \left( \sqrt{\frac{(z - f_0)R^2}{\delta}} \right) \right) \quad (1.5)$$

$$= \frac{1}{c} \left( z + \frac{(z - f_0)R^2}{\delta \cdot 2z} - \frac{R^2}{2\delta} \ln \left( 1 + \frac{z - f_0}{f_0} \right) \right) \quad (1.6)$$

In figure 1.3 the axiparabola can be seen on the left.

## 1.4 Spatio-temporal control

While the axiparabola allows for spatial control over the focal region, one can not steer when it arrives at the place. The time just follows equation 1.5 and does not have more parameters. However, because the focus length depends on  $r$  and, therefore, the light forming the focus at each  $z$  coordinate comes from a different radius  $r$  this behavior can be modified using a stepped mirror made up of flat, concentric rings of mirror surface that are at different depths half a wavelength apart, a so called radial group delay (RGD) echelon. By delaying the laser pulse in dependence of  $r$  by  $\Delta t = \tau_D(r)$  it is possible to adjust  $z = z(r(t)) = z(t)$  as needed by setting the function  $\tau_D(r)$  accordingly. This concept was proposed by Palastro et al [15] to solve the dephasing problem. Figure 1.3 shows this setup with the echelon on the right.

A pulse that has gone through both the RGD echelon and then the axiparabola is called a (ultrafast) flying focus pulse. Ambat et al [4] managed to achieve foci moving almost arbitrarily fast along the focal line with this technique.

Our goal for this work was to replicate this and make the flying focus laser pulse available in the PICOnGPU simulation software to make LWFA simulations with it possible.

# Chapter 2

## Simulation tools

For this work laser pulses were only simulated. The following tools were used for this:

### 2.1 Lasy

Lasy[1] stands for LAser manipulations made eaSY. It is a python library designed to simulate laser pulses on basis of the axiprop library. With it one can initialise a laser pulse using one of the provided profiles or from an array or file. Lasy offers a range of optical elements that can be applied to the pulse. One can then propagate the laser pulse by some distance. The standard propagation method uses axiprop, which has an angular spectrum propagator. Lasy is also currently developing other propagation methods.

In lasy the complex envelope  $\varepsilon$  of the electric field  $E_{pol}$ , defined by  $\text{Re}(\varepsilon \cdot e^{i\omega t}) = E_{pol}$ , is rasterised on a grid. There are two options to do this: Either using `dim = "xyt"`, a cartesian transversal grid and the time axis in the longitudinal direction, or using `dim = "rt"`, a 2D representation with radius and time on the axes and the option to have multiple azimuthal modes to represent not perfectly rotationally symmetrical lasers.

Lasy assumes, that the laser pulse will move at the speed of light  $c$  and moves its grid and its time axis along accordingly. It only ever shows the time relative to a standard speed-of-light-movement. This can be seen in figure 3.1 on the time axis.

### 2.2 openPMD

openPMD[10][2] stands for open (source) particle mesh data standard. It is a meta-data standard for mesh data like fields and particle data. The corresponding I/O library openPMD-api is used by a number of simulation software as well as by some measurement software. PICConGPU supports this format both through the openPMD plugin for output, in its checkpoints and as a laser source. Lasy also offers functions to import and export laser data in this file format. The two interpret the format differently, however, so they can not easily communicate in this way. Part of this work was to bridge that gap.

### 2.3 PICConGPU

PICConGPU[5][3] is a Particle-In-Cell simulation software that is being developed mainly at the HZDR. Being a PIC simulation it divides the simulation space into cells which each contain a field value and

some number of particles. For every time step it propagates the fields according to the Maxwell equations and pushes the particles along following their momentum and with a correction from interactions from the fields. Many interactions between particles as well as between particles and fields are modeled.

## 2.4 Additional modules

The following additional python modules were developed for this work. For a full documentation please go to the modules themselves on github at [12].

### 2.4.1 Module full\_field

The module `full_field` acts as an add-on to Lasy for this work. Among other things it bridges the gap between Lasy and PICConGPU by providing the function

```
full_field.laser_to_openPMD(laser, filename)
```

It saves the full electric field of the laser pulse into an openPMD-compatible file that PICConGPU can read. Because Lasy only calculates the complex envelope  $\varepsilon$  of the field this full electric field needs to be calculated first. While Lasy does offer a function for this, namely `lasy.utils.laser_utils.get_full_field(laser)`, it only calculates a 2D cut through the electric field, even if the laser calculation happened in 3D. Therefore in this module a similar function is implemented:

```
full_field.get_full_field(laser)
```

Parts of this function were taken from the Lasy implementation: If necessary the field envelope is interpolated to allow for more points in the propagation direction to more properly resolve the wavelength of the laser. Then it applies a phase of  $\phi = \exp(i\omega_0 t)$  and takes the real part to obtain the full electric field. The new function, however, calculates the 3D field if the laser is already 3D. It also offers some other options, see in the documentation. It is, for example, possible to calculate the field for only the central region of the laser pulse. This is useful because after focusing the laser pulse the Lasy laser object still has the field far out of the actual focused pulse.

After calculating the electric field the `laser_to_openPMD` function calls the function

```
full_field.write_to_openpmd_file(directory, filename, array, extent)
```

It writes an openPMD-compatible file to the specified location containing the array data, in this case the full electric field. Parts of its implementation are taken from the Lasy function `lasy.utils.openpmd_helper.write_to_openpmd_file` and other parts from the PICConGPU friendly implementation of `PrepRoutines.save_to_OpenPMD` from PICConGPU's INSIGHT data incorporation by Dietrich [8]. It was necessary to implement a new function for this because Lasy can only save an openPMD-compatible file containing the complex laser envelope with which PICConGPU can not work. To save on memory space, especially when loading the file into a GPU for a PICConGPU simulation, the data is stored in single precision float. It is also possible to only store every  $n$ th data point transversally to save more memory space.

Importantly, the function `laser_to_openPMD` is also able to generate and then save the field of a laser that has been simulated in cylindrical coordinates in Lasy. It does offer some more options as well, among them the option to display the field that has been saved to the file on a symlog plot. This can be seen in figure 2.2. To just calculate and display the electric field of the laser pulse there also is the function

```
full_field.show_field(laser)
```

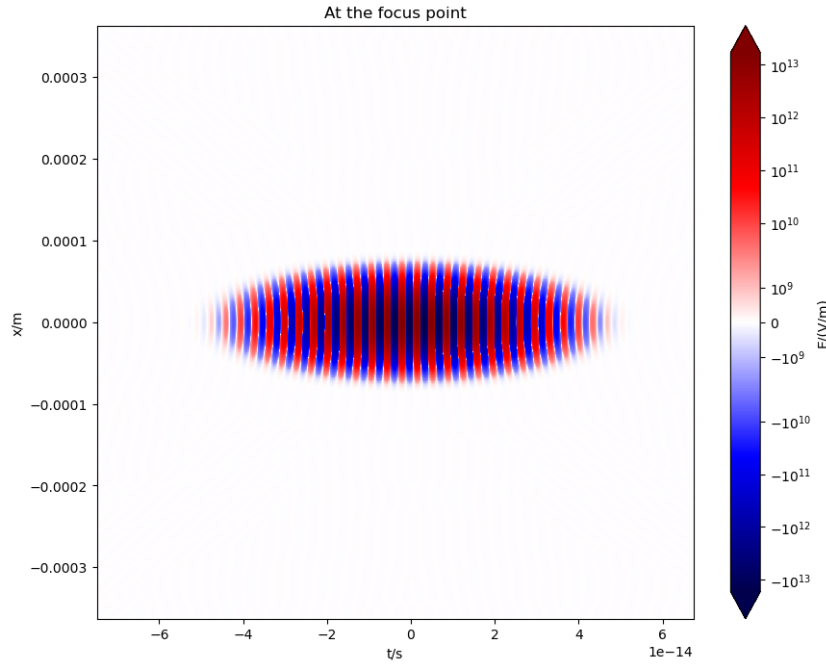


**Figure 2.1:** Full electric field of a gaussian laser pulse at its focus, according to a Lasy simulation.

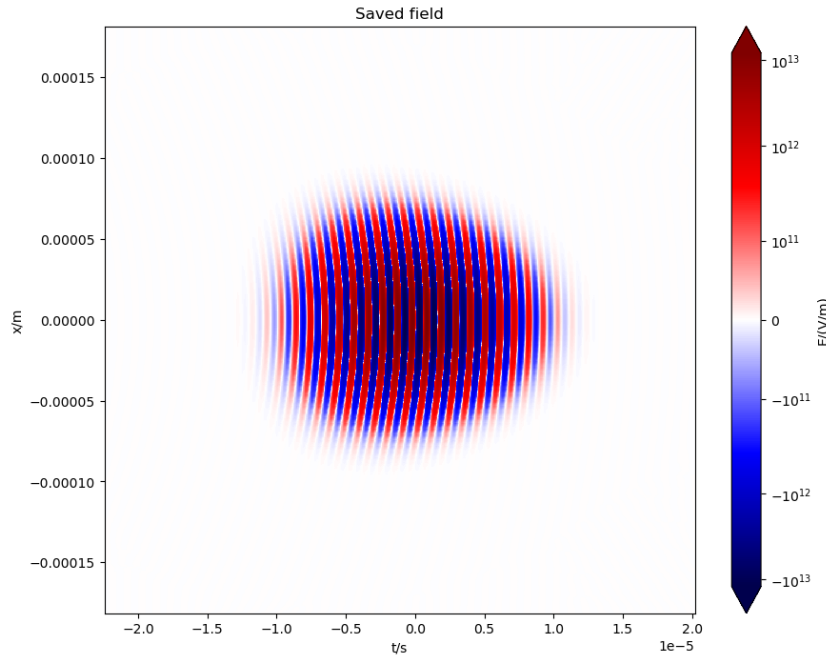


**Figure 2.2:** The field that has been saved as an openPMD-compatible file after Lasy simulation, one Rayleigh length before the focus.

An example of such a plot can be seen in figure 2.1. The module contains a few more functions that were useful when handling the Lasy laser and that were not available to Lasy natively.

#### 2.4.2 Module radialGroupDelay

The module `radialGroupDelay` mainly offers an implementation of the radial group delay echelon as a Lasy optical element. It can be applied to a laser as follows:

```
radialDelay = radialGroupDelay.RadialGroupDelay(tau_D, lambda0)
```

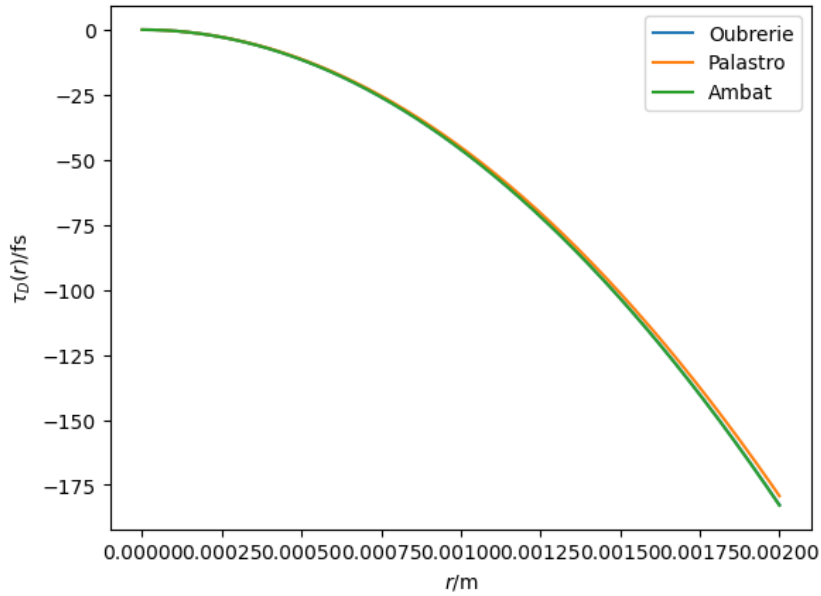


**Figure 2.3:** The three different  $\tau_D(r)$  for  $v_f = 1.02c$ , according to Oubrerie [14], Ambat [4] and Palastro [15]

```
laser.apply_optics(radialDelay)
```

It requires a function `tau_D(r)`, that describes by how much the pulse should be delayed, depending on the radius  $r$ , and the main wavelength of the pulse  $\lambda_0$ . It applies a radially dependent phase according to the following equation taken from Ambat et al [4] eq (11).

$$\phi_D^{ech}(\omega, r) = -\frac{2\omega}{c} \left\{ \frac{1}{4} \lambda_0 \left[ \text{ceil} \left( \frac{c\tau_D(r)}{\lambda_0} \right) + \text{floor} \left( \frac{c\tau_D(r)}{\lambda_0} \right) \right] \right\} \quad (2.1)$$

The stepped shape of the echelon is important to keep the wave fronts straight so that the pulse does not get defocused in any way.

To determine what the function  $\tau_D(r)$  should be, the papers [4], [15] and [14] offer three different differential equations but only one of them, Oubrerie et al [14], offers a solution to the equation. The module contains all three options as functions depending on the desired speed of the focus and the used axiparabola:

```
radialGroupDelay.tau_D_const_v(r, v, axiparabola)
radialGroupDelay.tau_D_integrated_ambat(r, v, axiparabola)
radialGroupDelay.tau_D_integrated_palastro(r, v, axiparabola)
```

In two cases the differential equations are numerically integrated, the third is implemented as is. To use these one can, for example, use `functools.partial` to define the desired focus velocity `v` and the used `axiparabola` before setting up the `RadialGroupDelay`.

All these functions were described in the papers as making the focus point of the axiparabola laser travel at some fixed speed that can be set arbitrarily, as long as it is close to the speed of light ( $v = v_0 + c$  with  $|v_0| \ll c$ ). To ensure these equations all described the same function  $\tau_D(r)$  figure 2.3 shows them in comparison. They are very similar.

Because an important usecase of this setup is LWFA, the module also provides a function that will return a velocity of the focus that should result in a propagation with vacuum light speed in a plasma:

```
radialGroupDelay.v_plasma(lambda0, n_e)
```

It depends, like the optical index of plasma, only on the laser wavelength  $\lambda_0$  and the electron density  $n_e$ .

### 2.4.3 Module axiparabola\_theory

The module `axiparabola_theory` is a collection of functions for theoretical calculations about the axiparabola and a laser pulse in its focal region. This theory is taken from Ambat et al [4]. Among the functions this module offers are implementations of equations (1.3), (1.4) and (1.5). Because it is important when dealing with PICConGPU simulations the parameters can not only be calculated in dependence of the radius  $r$  or the distance along the optical axis  $z$  but also in dependence of the arrival time of the focus point  $t_f$ . To do this it is necessary to invert equation (1.5) numerically.

The axiparabola that Lasy provides follows equation (1.2) and with the Smartsev et al [16]. Because they are slightly different (see section 5.2) the module also offers an alternative axiparabola implementation following Ambat et al [4].

### 2.4.4 Module showdata

The module `showdata` contains functions to display metadata and data from openPMD-compatible files and calculate pulse parameters from this data. The main function of the module is

```
showdata.show_file(filename)
```

This function displays the field that is stored in the file at `filename`. It offers the option to use all the following functions in the module. They can, however, be used independently as well. It also offers a variety of other options to modify what the output will look like.

The fields are displayed using the following function, which is also used by `full_field.show_field`:

```
showdata.show(array, extent)
```

This function plots the contents of `array` on a symlog-plot and offers a variety of options to change the appearance of the result. The plot may look similar to figure 2.4.

The next function in the module is:

```
showdata.show_metadata(filename)
```

This will display all the metadata that describes the fields and particles in the file.

The last two functions offer to calculate parameters of the pulse:

```
showdata.show_w()
```

and

```
showdata.show_lpeak()
```

These calculate the pulse waist and the longitudinal point of the peak, respectively.

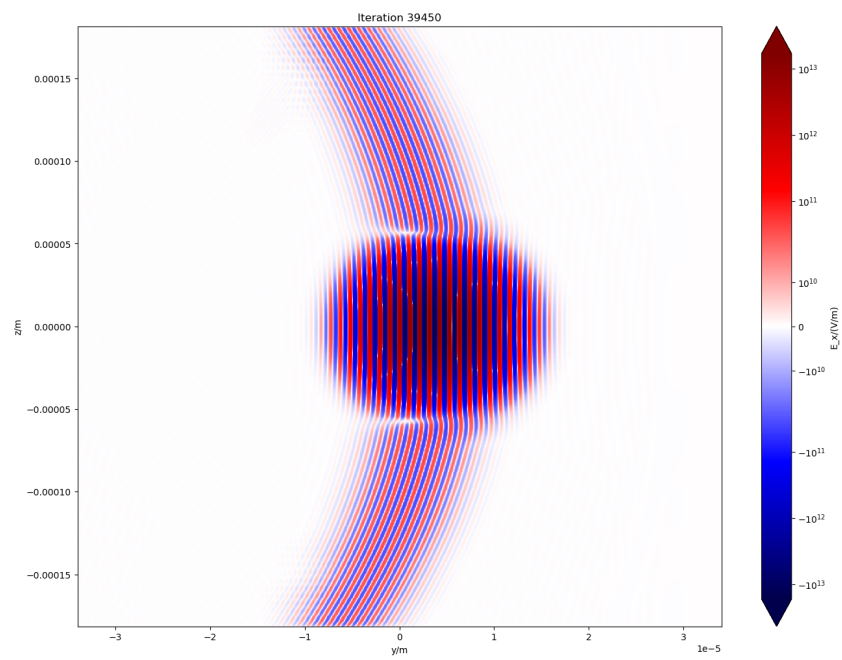


**Figure 2.4:** Gauss pulse at its focus point according to the PIConGPU simulation.

# Chapter 3

## Gaussian pulses in Lasy

The Lasy library offers functionality to generate, modify and propagate a laser pulse. The documentation can be found at [1].

### 3.1 Testing Gaussian pulses

A Gaussian laser pulse is one of the simplest and well known pulse shapes. It is, therefore, an important test case. The Gaussian pulse is defined by the main wavelength  $\lambda_0$ , the beam waist at the focus  $w_0$  and the pulse duration  $\tau$  as well as the maximum amplitude  $A$  and the polarisation direction  $\hat{e}_{pol}$ . At the focus the electric field looks like

$$\vec{E}(r, t) = A \hat{e}_{pol} \cdot e^{i\omega_0 t} \cdot e^{-\frac{r^2}{w_0^2}} \cdot e^{-\frac{t^2}{\tau^2}} \text{ with } \omega_0 = \frac{c}{2\pi\lambda_0}. \quad (3.1)$$

Because Lasy only uses the complex envelope of the laser field a Gaussian laser initialised in it has a field following

$$\varepsilon(r, t) = A \cdot e^{-\frac{r^2}{w_0^2}} \cdot e^{-\frac{t^2}{\tau^2}}. \quad (3.2)$$

The result of the propagation, displayed by `laser.show()`, can be seen in figure 3.1. Two parameters of the laser pulse after its propagation are of particular interest in this work: the beam waist  $w$  and time of arrival of the pulse  $t(z)$ .

The beam waist theoretically follows the relation

$$w(z) = w_0 \sqrt{1 + \left(\frac{z}{z_R}\right)^2} \text{ with } z_R = \frac{\pi w_0^2}{\lambda_0}. \quad (3.3)$$

Here  $z$  is measured from the focus. The lasy function `lasy.utils.laser_utils.get_w0(laser.grid, laser.dim)` can be used to calculate the beam waist of a given laser pulse. As one can see in figure 3.2 on the left the two give very similar results.

The time of arrival obviously follows the relation  $t(z) = \frac{z}{c}$ . In figure 3.2 on the right the deviation from this relation is shown and it turned out to be very little. The measurement was done with a function from the module `full_field`: `full_field.get_tpeak(laser)`

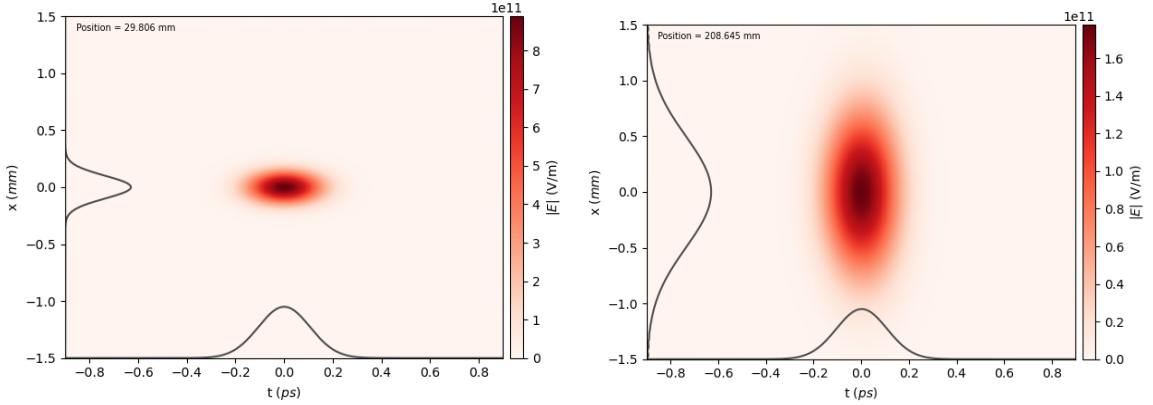


**Figure 3.1:** Gaussian pulse newly generated at the focus (left) and propagated  $6z_R$  (right) in Lasy.

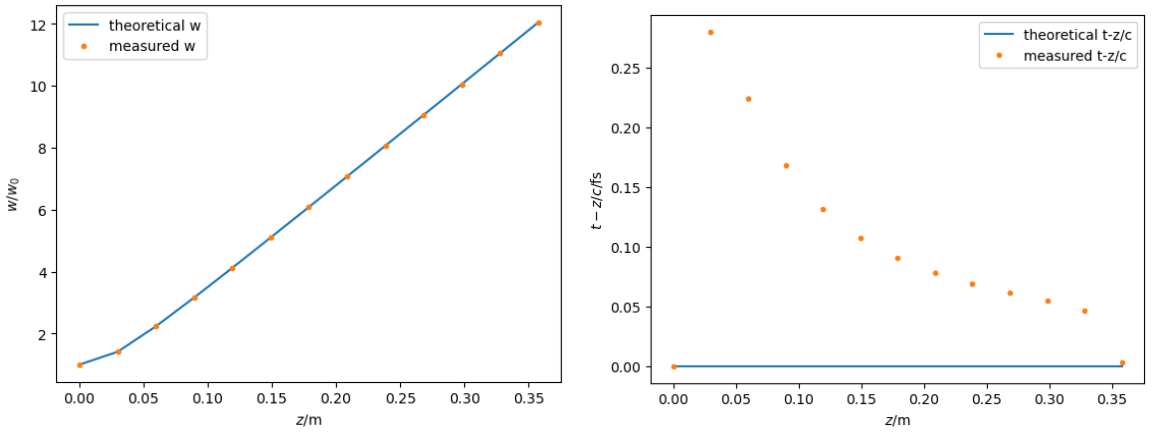


**Figure 3.2:** The beam waist  $w(z)$  (left) and the time difference  $t - \frac{z}{c}$  (right) compared to their respective theoretical values of a gaussian pulse initialised in the focus and propagated in Lasy. For comparison: the pulse duration was in this case  $\tau = 10\text{fs}$ .

## 3.2 Gaussian pulse and parabolic mirror

To generate a pulse for PICOnGPU simulations a Gaussian laser pulse with an initial beam waist of  $w_0$  was reflected by a parabolic mirror of focus length  $f$ . The pulse can be seen in figure 3.3 on the left side. To save on space in the RAM and on compute time while gaining precision the laser was simulated in cylindrical coordinates using the `dim = "rt"` option for Lasy lasers. This assumes, that the laser is radially symmetric (which should be the case here, because both the laser and the mirror have this symmetry) but the computer can handle a simulation with more than 10'000 points transversally.

From the parabolic mirror the laser propagated to one Rayleigh length  $z_R$  before the focus by a distance of  $l = f - z_R = f - \frac{\pi w_0^2}{\lambda_0}$  with  $w_0 = \frac{f\lambda_0}{w\pi}$ . Using the module `full_field` the electric field of the laser was saved to an openPMD-compatible file. The goal was to feed it into PICOnGPU one Rayleigh-length from the focus and then simulate it in through the focus point to one Rayleigh-length beyond it. In figure 3.3 the pulse now is shown on the right. The saved field can be seen in figure 2.2. To verify the Lasy propagation, the laser propagated into the focus and out of it again by a rayleigh length in Lasy. The beam waist at the focus was consistent with the theoretical value of  $w_0$ . The field at the focus is also shown in figure 2.1.

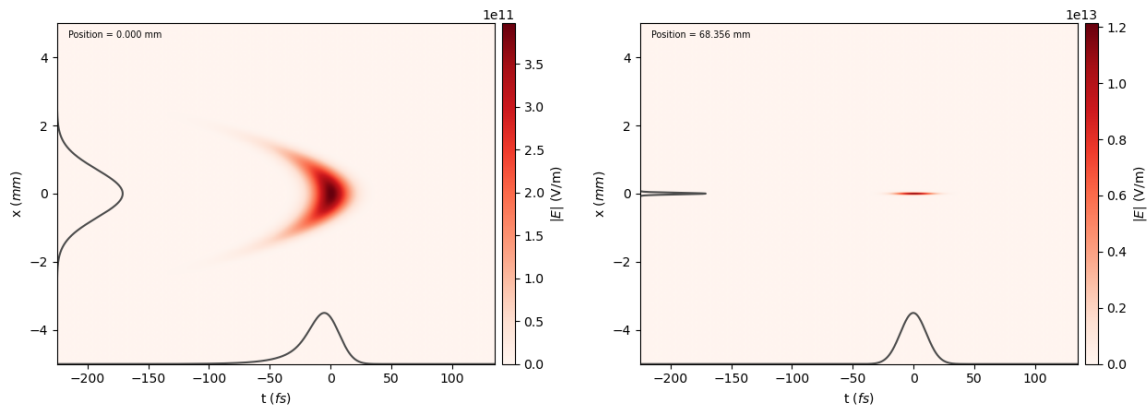


**Figure 3.3:** The laser pulse in the near field of the parabolic mirror (left) and in the far field, one Rayleigh length before the focus (right), simulated in Lasy.

## Chapter 4

# Lasy pulses in PICoGPU

To use the saved laser pulse from the Lasy propagation in a PICoGPU simulation PICoGPU's incident-Field.param file needs to be adjusted to use profiles::FromOpenPMDPulse. The propagation direction in the file must be set to "z" and the mesh name to "E". In order for the file to fit on the GPUs, it is important to change the parameter reservedGpuMemorySize in the file memory.param to accomodate the file's size in addition to what is already required here.

### 4.1 Courant-Friedrich-Levy (CFL) condition

Dietrich [8], who implemented the profiles::FromOpenPMDPulse, showed that it is important, that in the file simulation.param the time step is the same (or very close to the same) as the time step in the saved laser pulse. (This can easily be achieved by setting the `forced_dt` option to that same time step when calling the function `full_field.laser_to_openPMD` to generate the laser file in Lasy.) However, because it may be necessary to change the other parameters in the simulation.param file to be able to fit the laser pulse into a reasonable amount of cells it is important to remember to check the CFL-condition. The size of the simulation cells ( $\Delta x$ ,  $\Delta y$ ,  $\Delta z$ ) needs to be in the following relation with the time step  $\Delta t$  (see [3]):

$$c\Delta t < \frac{1}{\sqrt{\frac{1}{\Delta x} + \frac{1}{\Delta y} + \frac{1}{\Delta z}}} \quad (4.1)$$

However, the values on both sides of the inequality should be close to one another:

$$c\Delta t = \frac{\xi}{\sqrt{\frac{1}{\Delta x} + \frac{1}{\Delta y} + \frac{1}{\Delta z}}} \quad \text{with } \xi \approx 0.995 \quad (4.2)$$

For this purpose the module `full_field` contains the following function:

```
full_field.cfl_condition()
```

It returns the ideal time step for the specified cell size. If a time step is specified it will print how far off it is.

If the deviation between the used and the ideal time step is less than 5% the PICoGPU simulation will work without major problems [3].

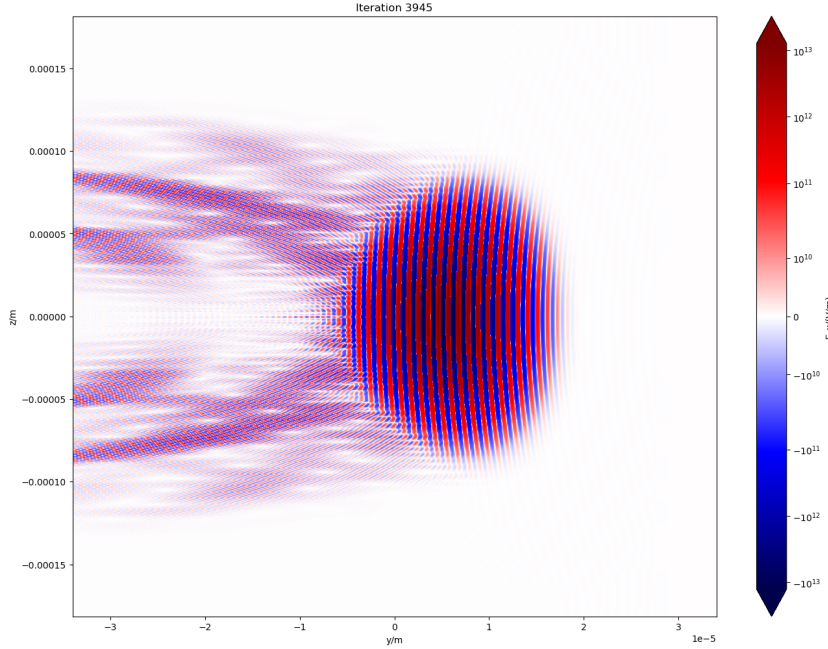


**Figure 4.1:** The laser pulse propagating into the PICoNGPU simulation volume.

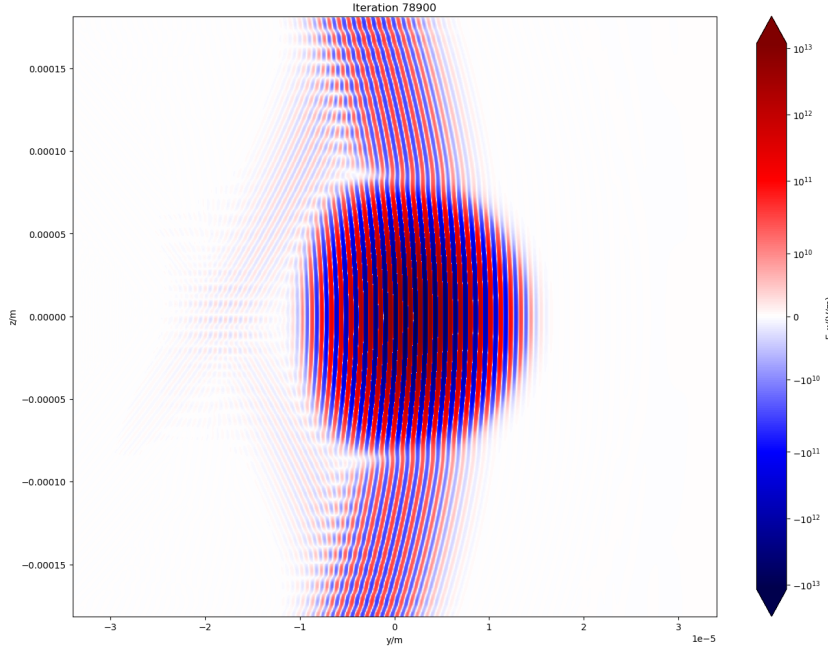


**Figure 4.2:** The laser propagated one Rayleigh length after the parabola focus in PICoNGPU.

## 4.2 Comparitative test with the Gauss laser

The laser pulse in the file (see figure 2.2) can be fed into PICoNGPU and simulated. Figure 4.1 shows the pulse as it enters the simulation volume. It is still almost a Rayleigh length away from the focus point. Behind the pulse there are some artifacts from the field initialisation method. These are a known issue of the simulation, see [17]. They can even move faster than light speed, as can be seen in figure 2.4 at the focus where they have moved along significantly. Ignoring those for the moment, however, the waist of the pulse can be measured using `showdata.show_w()` and at the focus the value is very similar to the calculated  $w_0$  from section 3.2. After a propagation one Rayleigh length past the focus the pulse

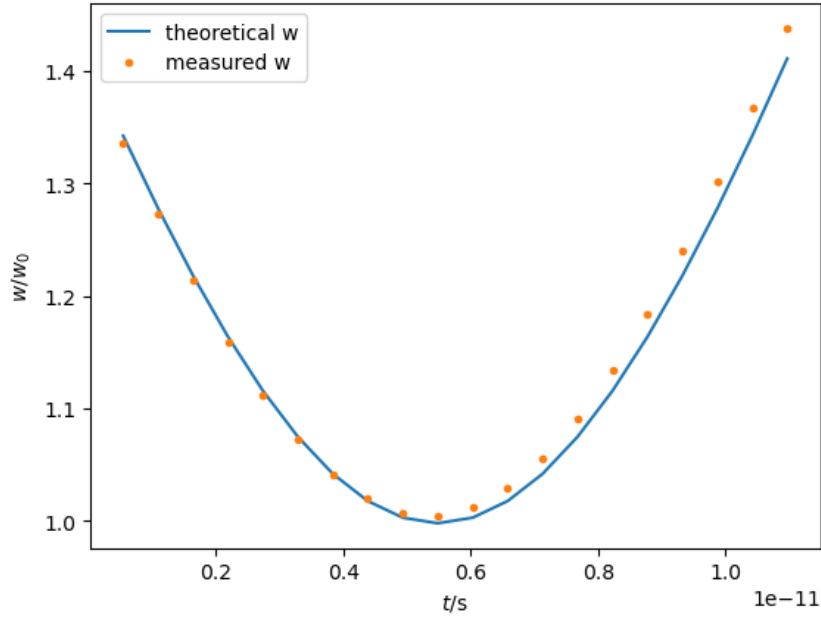


**Figure 4.3:** The width of the gaussian pulse over time, according to the PIConGPU simulation.

looks like in figure 4.2. Here the waist is a lot larger again. It develops over time as can be seen in figure 4.3. Here the focus is in the middle and the plot shows the propagation by one Rayleigh length in each direction. It also shows the expected values from equation 3.3 for comparison. They follow a very similar development, though towards the end the simulation artifacts skew the values to be larger. They can achieve this because the values of  $w$  are calculated statistically here.

One can also see the shape of the wave fronts, always curved towards the focus point. At the focus point (figure 2.4) they are flat. [energy in artifacts?]

# Chapter 5

## The flying focus laser

The previous sections have proven that the methods work. Now they can be applied to the ultrafast flying focus laser.

### 5.1 Testing the radial group delay

To test the functionality of the radial group delay echelon (RGD) implementation described in section 2.4.2 a laser pulse was reflected by the RGD and then propagated to different distances. Figure 5.1 shows, that the shape of the pulse barely changes after the echelon, which is what should happen. There are some artifacts from the simulation but they appear to be minor. Figure 5.2 shows the shape of the pulse after the RGD after propagation for different distances. It is clearly visible, that for the most part the shape does not change after the RGD. Only at  $r = 0$  and at the edge there are some differences. The center is an effect of the artifact visible in figure 5.1 on the right. Because the simulation ran on a radial grid it always generates artifacts at  $r = 0$ . At the edge the intensity has dropped so much that noise from the simulation begins to take effect. In conclusion, the RGD works as intended.

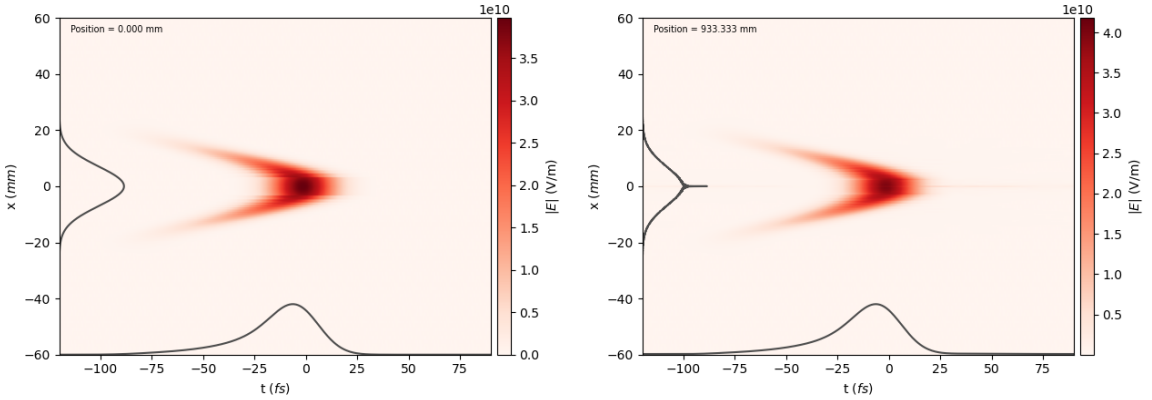


**Figure 5.1:** The laser pulse in the near field of the radial group delay echelon (left) and propagated 93 cm (right), simulated in Lasy.

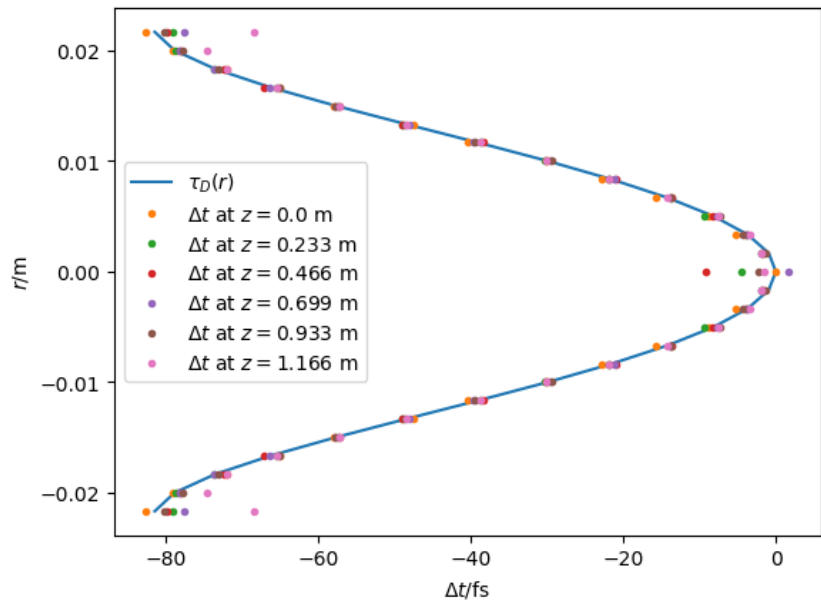


**Figure 5.2:** The shape of the pulse after the RGD, compared to the function  $\tau_D(r)$ , simulated in Lasy.

## 5.2 Testing the axiparabola

Lasy offers an axiparabola object natively. One can just apply one to a laser pulse like this:

```
axiparabola = lasy.optical_elements.Axiparabola(f0, delta, R)
laser.apply_optics(axiparabola)
```

Figure 5.3 shows the laser pulse after the axiparabola is applied as well as after being propagated to the beginning of the focus. The full electric field at the focus is shown in figure 5.4. Because the original pulse in this case was not a Gaussian pulse but a super-Gaussian pulse of order 6 transversally the shape at the focus is not a gaussian pulse either. It is instead close to a sinc function, as one would expect. Figure 5.6 shows the results of a simulation where the laser propagated past the focus point through the focal region. They are compared to theoretical calculations according to equations (1.4) and (1.5). The module `axiparabola_theory` (see section 2.4.3) was used to calculate the values to compare to. As figure 5.5 shows were Ambat et al able to see the behavior described by the equations 1.4 (see image (c)) and 1.5 (see image (d)). This is clearly not what can be seen in the results here in figure 5.6.

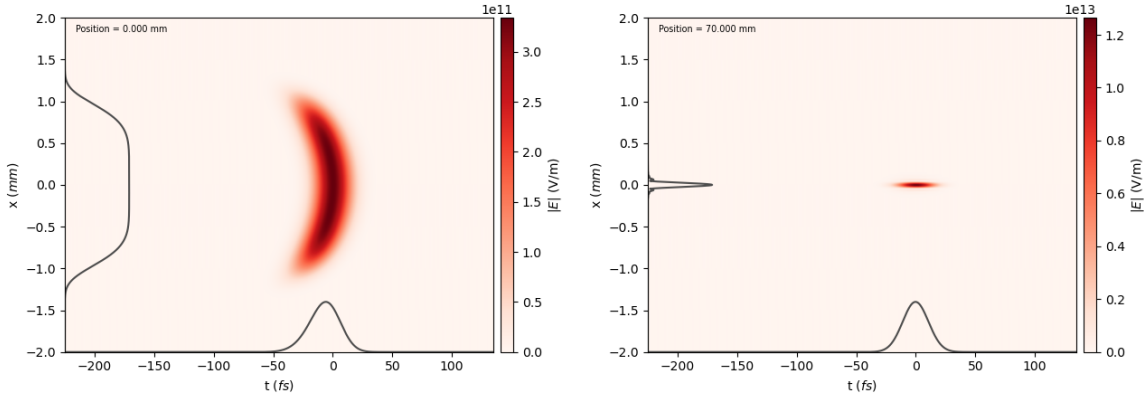


**Figure 5.3:** The laser pulse in the near field of the axiparabola (left) and in the far field at the focus (right), simulated in Lasy.

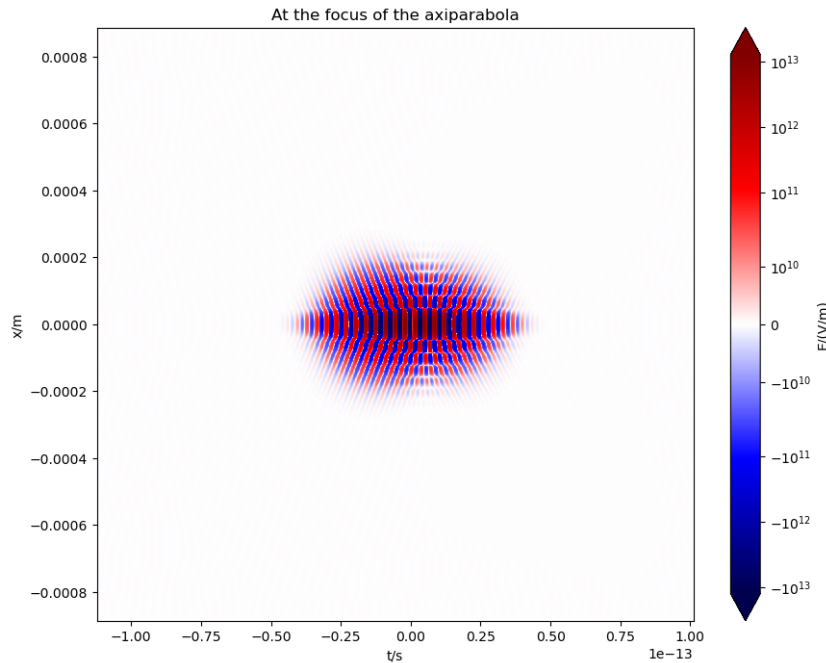


**Figure 5.4:** The full electric field of the pulse at the focus of the axiparabola according to a Lasy simulation.

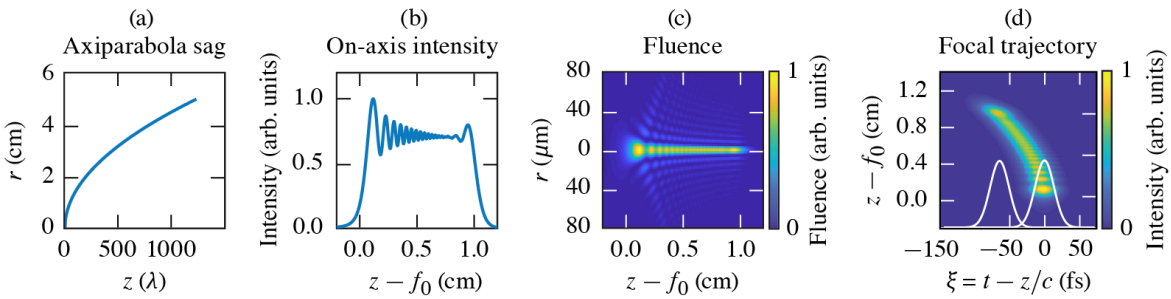


**Figure 5.5:** Graphic taken from Ambat et al [4] showing their axiparabola simulation. (a) the shape of the axiparabola, the so called sag function. (b) The on-axis intensity of the laser pulse as the focus moves along  $\delta$ . (c) A plot showing the beam waist  $w$  of the pulse as it travels the focal region. It roughly follows equation (1.4). (d) A plot showing , that the arrival time of the pulse follows equation (1.5).

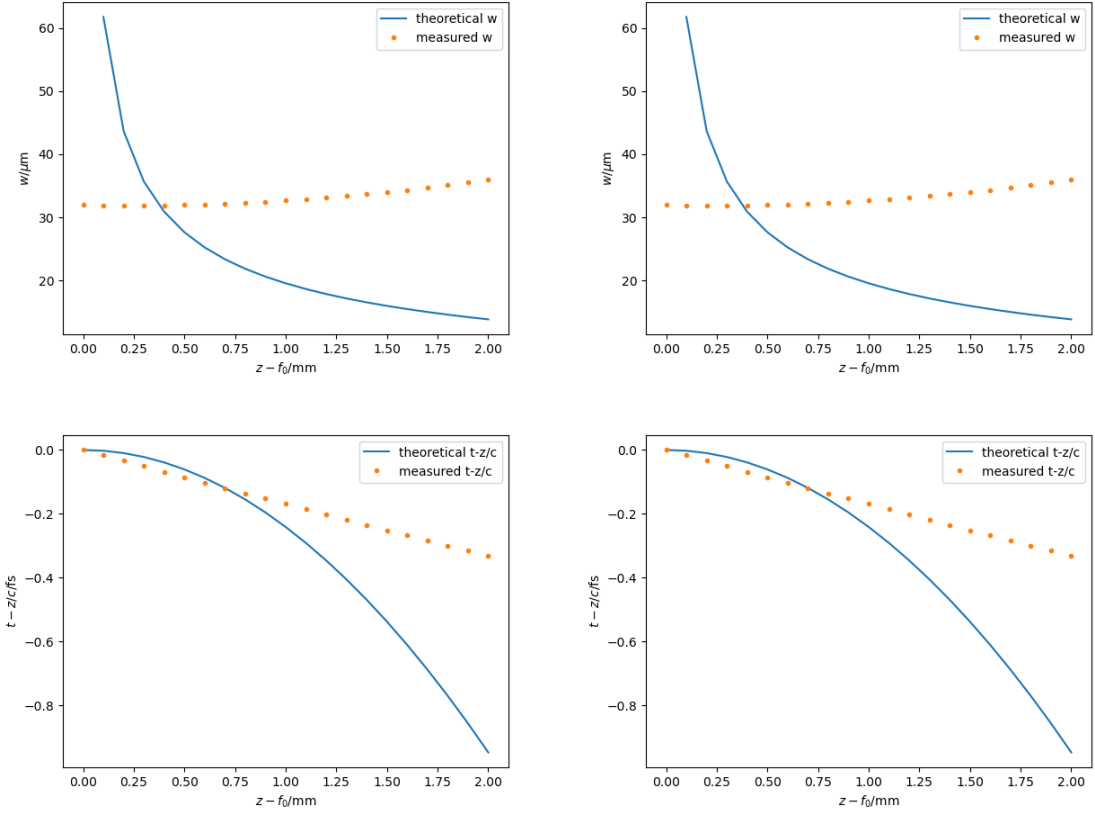


**Figure 5.6:** The beam waist  $w$  (top) and the relative time shift  $\Delta t = t - \frac{z}{c}$  (bottom) over the focal region  $\delta$  of the axiparabola according to a Lasy simulation. The left side shows a propagation from one point to another and the right shows a direct propagation from the axiparabola to each point.

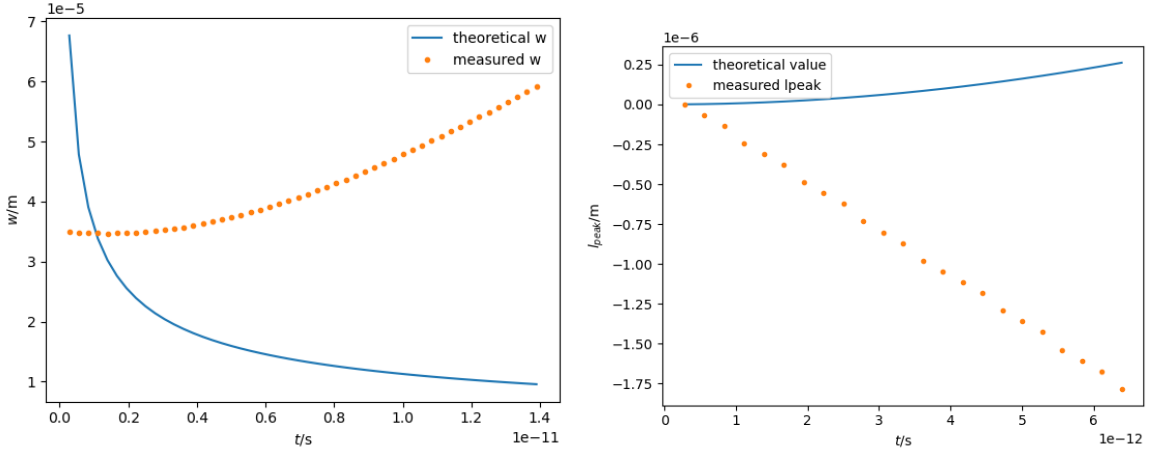


**Figure 5.7:** The beam waist  $w$  (left) and peak position  $z - ct$  (right) of the axiparabola laser according to the PICConGPU simulation.

The naive way of doing such a simulation in lasy is to just propagate the laser to a point, measure  $w$  and  $\Delta t$  and then propagate it further from there. The results of that are shown on the left of figure 5.6. Because measurement and theory clearly do not align here I tried to propagate the laser pulse to each point separately from the axiparabola to avoid compounding errors. The results of that test are shown on the right of the figure and are clearly in line with the plots on the left. These possible compounding errors of the propagation can therefore be excluded as the main source of the difference

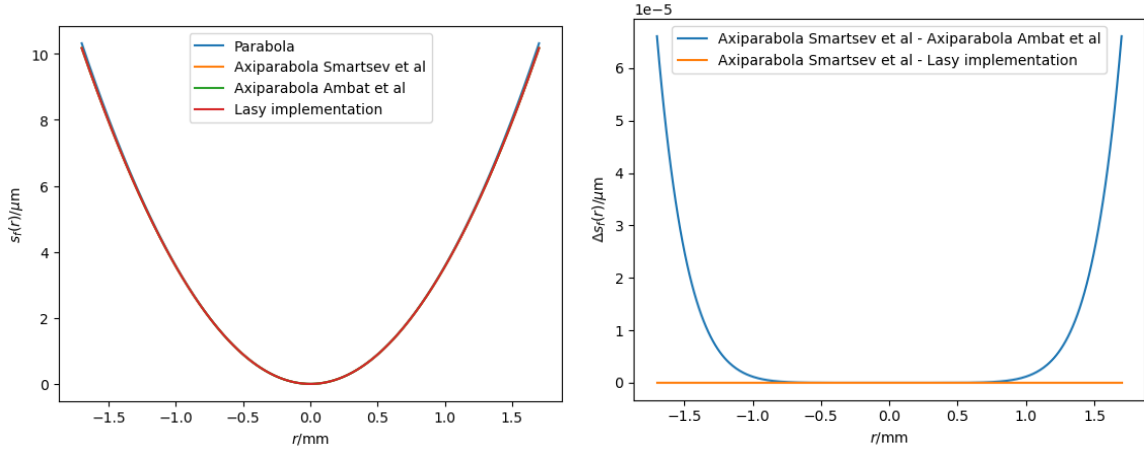


**Figure 5.8:** The shape of the axiparabola. Left: Smartsev [16] and Ambat [4] compared with the Lasy implementation [1] and a regular parabolic mirror. Right: A relative comparison of the same sag functions  $s_f(r)$  for the axiparabola.

between measurement and theory.

In order to exclude another possible problem the same propagation simulation was also run in PICConGPU. The results are shown in figure 5.7. The simulation methods are extremely different from one another: Lasy works in fourier space using angular spectrum propagation, PICConGPU simply integrates the Maxwell equations. Still, the results are of similar nature: The beam waist goes up instead of down and the focus does not move as expected either. The propagation method within the focal region is clearly not the problem here.

Because both simulation methods have already been tested with the known Gauss-laser in sections 3 for the lasy propagation and 4 for the PICConGPU propagation the methods to propagate to the focus and import the pulse to PICConGPU are unlikely to be the problem here.

The remaining options for causing the differences between theory and measurement are the axiparabola itself or the theory being incorrect. For this reason figure 5.8 shows a comparison of the sag functions described in the different papers, the one used in Lasy and a normal parabolic mirror. They are all very similar.

### 5.3 The complete assembly

Combining the two elements and applying them to the laser one should get a flying focus laser. Figure 5.9 shows, what this will look like for a desired focal velocity  $v_f = 0.98c$  or  $v_f = 1.02c$ . The field is now shaped quite different to what it was before, as can be seen in figure 5.10. It is no longer symmetrical in the propagation direction. However, the two plots look like mirror images of each other. This makes sense, as the peak of the pulse is supposed to be moving in opposite directions relative to the speed of light. Because the axiparabola cuts the pulse off at a specific radius  $R$  and the RGD introduces sudden jumps as well the defraction artefacts are more pronounced than before but they should be mostly physical.

The figures 5.11 and 5.12 show the results of lasy simulations with the flying focus assembly. Like in figure 5.6 a consecutive and a pointwise separate simulation are shown. Of course theoretical formula for the beam waist, equation 1.4, does not necessarily apply for this setup. First of all the beam waist is apparently larger in this case, according to the simulation. The curve is shown only for the lack of a better formula. However, the other diagram is of major importance here. The flying focus assembly is meant to make the focus point move at vacuum speed of light in the plasma of an LWFA chamber.

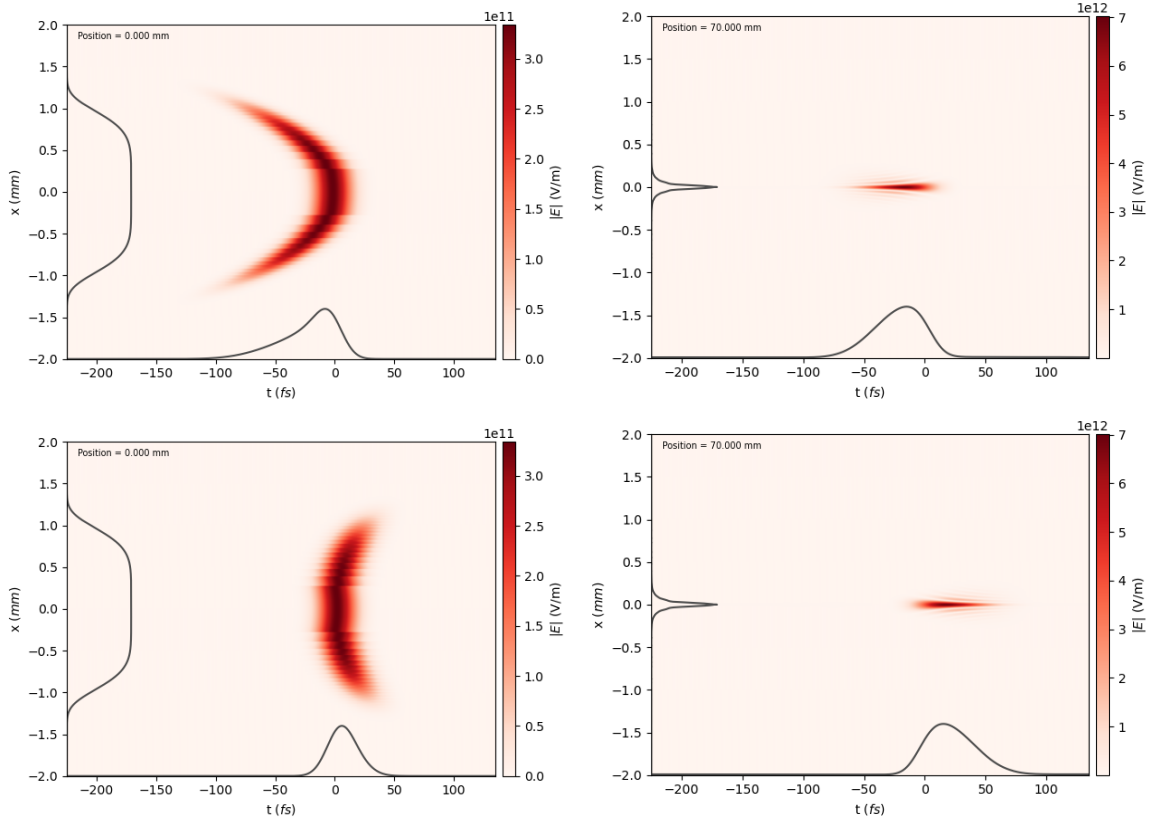


**Figure 5.9:** The laser pulse in the near field of the combined elements (left) and in the far field at the focus (right); designed for  $v_f = 1.02c$  (top) and for  $v_f = 0.98c$  (bottom); simulated in Lasy.

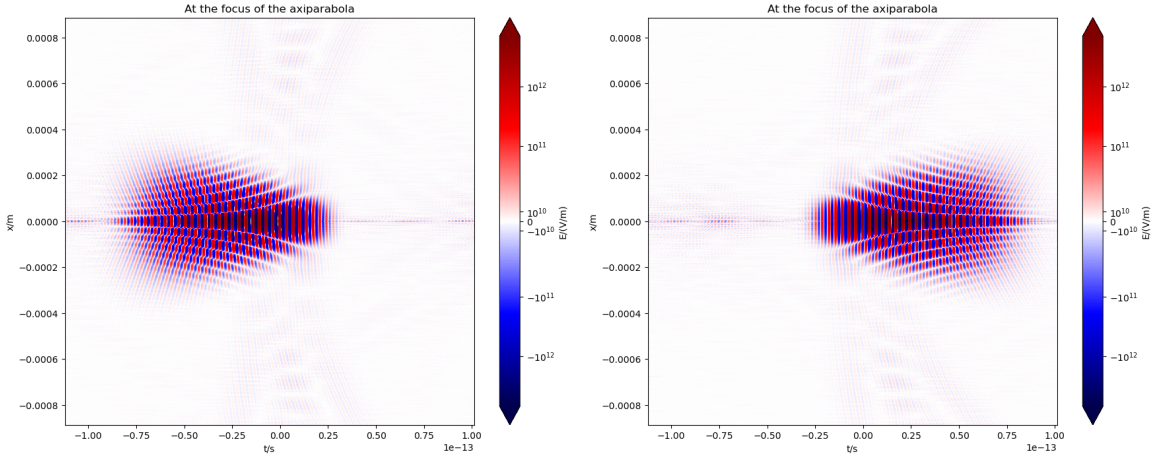


**Figure 5.10:** The electric field at the focus of the echelon axiparabola assembly, designed for  $v_f = 1.02c$  (left) and for  $v_f = 0.98c$  (right), simulated in Lasy.

For that the focus time must move like the theoretical lines in the bottom plots of the two figures. This is clearly not the case. The RGD did not manage to fix the problem with the axiparabola in the flying focus case.

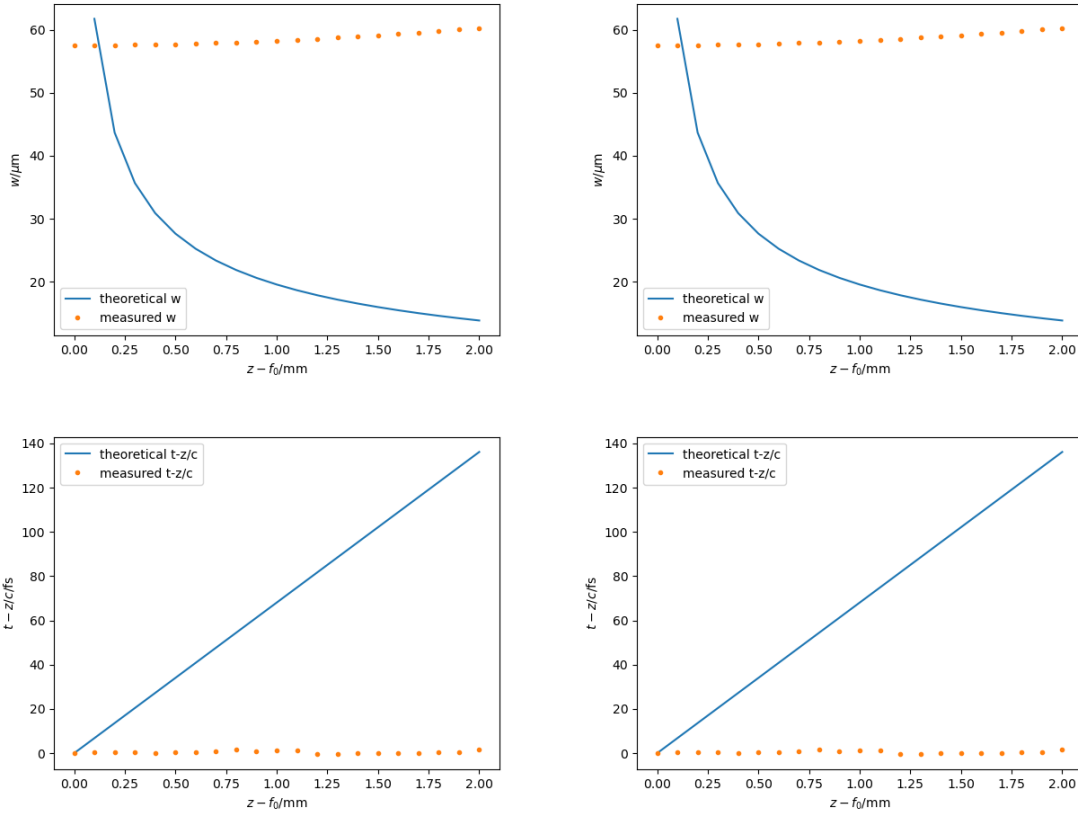


**Figure 5.11:** The beam waist  $w$  (top) and the relative time shift  $\Delta t = t - \frac{z}{c}$  (bottom) over the focal region  $\delta$  of the flying focus assembly for  $v_f = 0.98c$  according to a Lasy simulation. The left side shows a propagation from one point to another and the right shows a direct propagation from the axiparabola to each point.

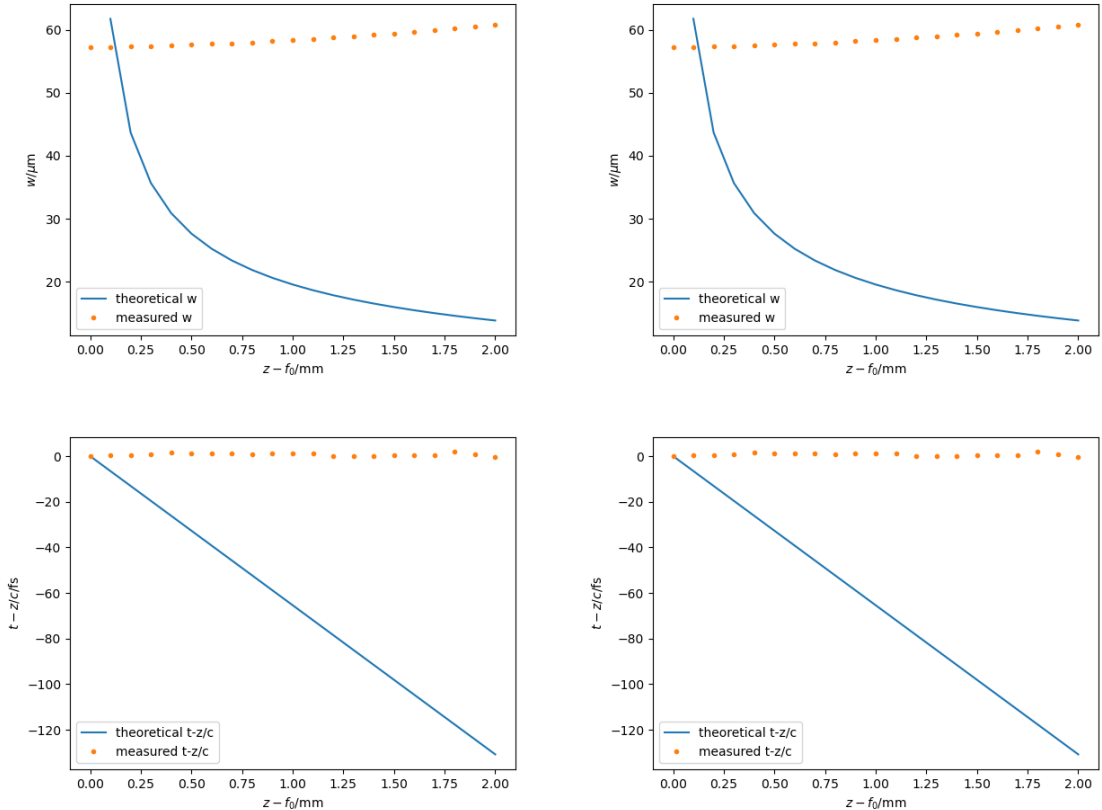


**Figure 5.12:** The beam waist  $w$  (top) and the relative time shift  $\Delta t = t - \frac{z}{c}$  (bottom) over the focal region  $\delta$  of the flying focus assembly for  $v_f = 1.02c$  according to a Lasy simulation. The left side shows a propagation from one point to another and the right shows a direct propagation from the axiparabola to each point.

## 5.4 Testing different propagators

One reason for the differences between theory and the previous simulations might still be the propagation of the laser from the axiparabola to its focus. In chapter 3 is shown, that the propagator works for simple Gaussian pulses but it could be that the pulse here is to complicated for it. Therefore the following other propagators were also tested. One can simply apply such a propagator after initialisation to a Lasy laser as follows:

```
laser.add_propagator(propagator)
```

However, at their current implementation at the time of writing these alternative propagators dont support lasers in cylindrical coordinates and only cartesian coordinates are usable. This has the disadvantage that it is a lot more memory intensive meaning it allows for fewer points transversally and longitudinally than previous simulations described in this work.

### 5.4.1 AngularSpectrumPropagator

### 5.4.2 FresnelChirpZPropagator

# Chapter 6

## Summary and Outlook

### 6.1 Summary

In conclusion I was able to use Lasy and PICConGPU in conjunction to simulate laser pulses by first generating the pulse in Lasy, potentially sending it through optical elements and propagating it for some distances, save it to an openPMD compatible file that PICConGPU can read and finally simulate the laser from the file in PICConGPU. The previous sections have shown that this will correctly portray simple gauss pulses and that the translation from one simulation method does not majorly change the outcome. I also managed to implement a working RGD echelon optical element that could be patched into the lasy library.

However, it was not possible to replicate the findings in other papers (Ambat et al [4] etc., see section 1.3) regarding the axiparabola and its far field. Therefore it was also not possible to generate a flying focus laser as it has been described.

### 6.2 Outlook

In the future people will be able to use this new framework to use more complicated laser setups for their PICConGPU simulations. Hopefully someone will be able to find the reasons for the descrepancy between the description of the axiparabola in the papers and the simulation results in this work.

(\*) There's more to explore here.

### 6.3 Code availability

All the code used in this work that I have written and mentioned here can be found on github at [12].

# Bibliography

- [1] Lasy 0.6.2 documentation. <https://lasydoc.readthedocs.io/en/latest>. Accessed october 2025.
- [2] openpmd 0.16.1 documentation. <https://openpmd-api.readthedocs.io/en/0.16.1>. Accessed october 2025.
- [3] Picongpu 0.7.0 documentation. <https://picongpu.readthedocs.io/en/0.7.0>. Accessed october 2025.
- [4] M. V. Ambat, J. L. Shaw, J. J. Pigeon, K. G. Miller, T. T. Simpson, D. H. Froula, and J. P. Palastro. Programmable-trajectory ultrafast flying focus pulses. *Optics Express*, 31(19), 2023.
- [5] M. Bussmann, H. Burau, T. E. Cowan, A. Debus, A. Huebl, G. Juckeland, T. Kluge, W. E. Nagel, R. Pausch, F. Schmitt, U. Schramm, J. Schuchart, and R. Widera. Radiative signatures of the relativistic kelvin-helmholtz instability. In *Proceedings of the International Conference on High Performance Computing, Networking, Storage and Analysis*, SC '13, pages 5:1–5:12, New York, NY, USA, 2013. ACM.
- [6] J. P. Couperus, R. Pausch, A. Köhler, O. Zarini, J. M. Krämer, M. Garten, A. Huebl, R. Gebhardt, U. Helbig, S. Bock, K. Zeil, A. Debus, M. Bussmann, U. Schramm, and A. Irman. Demonstration of a beam loaded nanocoulomb-class laser wakefield accelerator. *Nature Communications*, 8, 2017.
- [7] Alexander Debus, Richard Pausch, Axel Huebl, Klaus Steiniger, René Widera, Thomas E. Cowan, Ulrich Schramm, and Michael Bussmann. Circumventing the dephasing and depletion limits of laser-wakefield acceleration. *Physical Review X*, 9, 2019.
- [8] Fabia Dietrich. Implementation and validation of a method for using experimentally measured laser profiles in laser-plasma simulations with picongpu. Master's thesis, HZDR, TU Dresden, 2024.
- [9] A Hannasch, AL Garcia, M LaBerge, R Zgadzaj, A Köhler, JPC Cabadag, O Zarini, T Kurz, A Ferrari, M Molodtsova, L Naumann, TE Cowan, U Schramm, A Irman, and MC Downer. Compact spectroscopy of kev to mev x-rays from a laser wakefield accelerator. *Scientific reports*, 11, 2021.
- [10] Axel Huebl, Rémi Lehe, Jean-Luc Vay, David P. Grote, Ivo Sbalzarini, Stephan Kuschel, David Sagan, Christopher Mayes, Frédéric Pérez, Fabian Koller, Franz Poeschel, Carsten Fortmann-Grote, Angel Ferran Pou, Juncheng E, Maxence Thévenet, and Michael Bussmann. openPMD: A meta data standard for particle and mesh based data. <https://github.com/openPMD>, 2015.
- [11] A Irman, JP Couperus, A Debus, A Köhler, JM Krämer, R Pausch, O Zarini, and U Schramm. Improved performance of laser wakefield acceleration by tailored self-truncated ionization injection. *Plasma Physics and Controlled Fusion*, 60, 2018.

- [12] Edgar Marquardt. lasy\_incorporation. [https://github.com/Ehtyar/lasy\\_incorporation](https://github.com/Ehtyar/lasy_incorporation). Repository containing this work and all code written for it.
- [13] Kyle G. Miller, Jacob R. Pierce, Manfred V. Ambat, Jessica L. Shaw, Kale Weichman, Warren B. Mori, Dustin H. Froula, and John P. Palastro. Dephasingless laser wakefield acceleration in the bubble regime. *Sci. Rep.*, 13, 2023.
- [14] Kosta Oubrerie, Igor A Andriyash, Ronan Lahaye, Slava Smartsev, Victor Malka, and Cédric Thaury. Axiparabola: a new tool for high-intensity optics. *J. Opt.*, 24, 2022.
- [15] J. P. Palastro, J. L. Shaw, P. Franke, D. Ramsey, T. T. Simpson, and D. H. Froula. Dephasingless laser wakefield acceleration. *Phys. Rev. Letters*, 124, 2020.
- [16] Slava Smartsev, Clement Caizergues, Kosta Oubrerie, Julien Gautier, Jean-Philippe Goddet, Amar Tafzi, Kim Ta Phuoc, Victor Malka, and Cedric Thaury. Axiparabola: a long-focal-depth, high-resolution mirror for broadband high-intensity lasers. *Optics Letters*, 44, 2019.
- [17] Klaus Steiniger. Issue 5269 todo in laser refactoring. <https://github.com/ComputationalRadiationPhysics/picongpu/issues/5269>. Accessed october 2025.
- [18] T Tajima and JM Dawson. Laser electron-accelerator. *Physical Review Letters*, 43(4), 1979.

# List of Figures

1.1	PIConGPU simulation of laser wakefield acceleration. Displayed are the electrons, colored according to their energy $E$ , the electric field of the laser pulse $E_x$ and the on-axis accelerating field $E_y$ in blue. . . . .	7
1.2	Schematic of how an axiparabola focuses light into the focal region. Rays close to the optical axis are focused to a focus length of $f_0$ and rays far from the axis are focused closer to $f_0 + \delta$ . (a) On-axis case, (b) off-axis case. Image taken from Smartsev et al[16]. . . . .	8
1.3	Schematic of the flying focus setup. A flat laser pulse (a) is first reflected by the radial group delay echelon (b). It imparts a time delay onto the pulse without aberrations. The pulse (c) is then reflected by the axiparabola, which focuses the pulse (d) into the focal region $\delta$ (e), where it can theoretically drive a laser wakefield accelerator without dephasing. Image taken from Palastro et al [15]. . . . .	8
2.1	Full electric field of a gaussian laser pulse at its focus, according to a Lasy simulation. . . . .	12
2.2	The field that has been saved as an openPMD-compatible file after Lasy simulation, one Rayleigh length before the focus. . . . .	12
2.3	The three different $\tau_D(r)$ for $v_f = 1.02c$ , according to Oubrerie [14], Ambat [4] and Palastro [15]. . . . .	13
2.4	Gauss pulse at its focus point according to the PIConGPU simulation. . . . .	15
3.1	Gaussian pulse newly generated at the focus (left) and propagated $6z_R$ (right) in Lasy. . . . .	17
3.2	The beam waist $w(z)$ (left) and the time difference $t - \frac{z}{c}$ (right) compared to their respective theoretical values of a gaussian pulse initialised in the focus and propagated in Lasy. For comparison: the pulse duration was in this case $\tau = 10\text{fs}$ . . . . .	17
3.3	The laser pulse in the near field of the parabolic mirror (left) and in the far field, one rayleigh length before the focus (right), simulated in Lasy. . . . .	18
4.1	The laser pulse propagating into the PIConGPU simulation volume. . . . .	20
4.2	The laser propagated one Rayleigh length after the parabola focus in PIConGPU. . . . .	20
4.3	The width of the gaussian pulse over time, according to the PIConGPU simulation. . . . .	21
5.1	The laser pulse in the near field of the radial group delay echelon (left) and propagated 93 cm (right), simulated in Lasy. . . . .	23
5.2	The shape of the pulse after the RGD, compared to the function $\tau_D(r)$ , simulated in Lasy. . . . .	23
5.3	The laser pulse in the near field of the axiparabola (left) and in the far field at the focus(right), simulated in Lasy. . . . .	24
5.4	The full electric field of the pulse at the focus of the axiparabola according to a Lasy simulation. . . . .	24

5.5	Graphic taken from Ambat et al [4] showing their axiparabola simulation. (a) the shape of the axiparabola, the so called sag function. (b) The on-axis intensity of the laser pulse as the focus moves along $\delta$ . (c) A plot showing the beam waist $w$ of the pulse as it travels the focal region. It roughly follows equation (1.4). (d) A plot showing , that the arrival time of the pulse follows equation (1.5). . . . .	24
5.6	The beam waist $w$ (top) and the relative time shift $\Delta t = t - \frac{z}{c}$ (bottom) over the focal region $\delta$ of the axiparabola according to a Lasy simulation. The left side shows a propagation from one point to another and the right shows a direct propagation from the axiparabola to each point. . . . .	25
5.7	The beam waist $w$ (left) and peak position $z - ct$ (right) of the axiparabola laser according to the PIConGPU simulation. . . . .	25
5.8	The shape of the axiparabola. Left: Smartsev [16] and Ambat [4] compared with the Lasy implementation [1] and a regular parabolic mirror. Right: A relative comparison of the same sag functions $s_f(r)$ for the axiparabola. . . . .	26
5.9	The laser pulse in the near field of the combined elements (left) and in the far field at the focus (right); designed for $v_f = 1.02c$ (top) and for $v_f = 0.98c$ (bottom); simulated in Lasy. . . . .	27
5.10	The electric field at the focus of the echelon axiparabola assembly, designed for $v_f = 1.02c$ (left) and for $v_f = 0.98c$ (right), simulated in Lasy. . . . .	27
5.11	The beam waist $w$ (top) and the relative time shift $\Delta t = t - \frac{z}{c}$ (bottom) over the focal region $\delta$ of the flying focus assembly for $v_f = 0.98c$ according to a Lasy simulation. The left side shows a propagation from one point to another and the right shows a direct propagation from the axiparabola to each point. . . . .	28
5.12	The beam waist $w$ (top) and the relative time shift $\Delta t = t - \frac{z}{c}$ (bottom) over the focal region $\delta$ of the flying focus assembly for $v_f = 1.02c$ according to a Lasy simulation. The left side shows a propagation from one point to another and the right shows a direct propagation from the axiparabola to each point. . . . .	29



## **Erklärung**

Hiermit erkläre ich, dass ich diese Arbeit im Rahmen der Betreuung am Institut für Kern- und Teilchenphysik ohne unzulässige Hilfe Dritter verfasst und alle Quellen als solche gekennzeichnet habe.

Edgar Marquardt  
Dresden, December 9, 2025